2013

Solid-State Nuclear Magnetic Resonance Analysis of Cytosine-Methylated DNA Dodecamer

Caitlin A. Edmunds
Scripps College

Solid-State Nuclear Magnetic Resonance Analysis of Cytosine-Methylated DNA Dodecamer

A Thesis Presented

by

Caitlin A. Edmunds

To the Keck Science Department

Of Claremont McKenna, Pitzer, and Scripps Colleges

In partial fulfillment of

The degree of Bachelor of Arts

Senior Thesis in Biochemistry

December 10, 2012

TABLE OF CONTENTS

1 ABSTRACT

The interaction of deoxyribonucleic acid (DNA) and cellular proteins is absolutely central to any biological understanding of DNA replication, transcription, and even gene regulation. Because an incumbent protein interacts not only with the four bases but also the backbone phosphate groups of the nucleic acid, backbone dynamics directly pertain to an understanding of basic cell processes[5]. Studies have shown that DNA exists in a balance of two conformations, BI and BII, defined by the difference in their backbone torsion angles[6]. A given DNA sequence expresses a preference for either BI or BII, though both exist in most samples (and are presented as a ratio); factors affecting that ratio include flanking sequence and methylation[7]. When a DNA sample is methylated, which commonly occurs at a cytosine base, backbone dynamics at that site and perhaps even its neighbors are sometimes quenched[4, 8]. DNA methylation is implicated in cancer diagnosis by new studies focusing on hypermethylation in CpG islands[9, 10].

This thesis uses solid-state deuterium NMR to study the backbone dynamics of the Dickerson dodecamer, $[d(CGCGAATTCGCG)]_2$, which was the first synthetic B-form DNA sequence successfully crystallized (allowing for analysis in the solid state) and which contains the *Eco*RI binding site, GAATTC[11]. This molecule is a good model system because a massive amount of information has been gathered on it not only using NMR, both high-resolution and solid-state, but also using x-ray diffraction, electron paramagnetic resonance, and all-atom molecular dynamics simulation[4, 8, 12-17]. This thesis research attempts to show the quenching of methyl rotation due to a CH--OH bond. In order to begin NMR analysis, a mechanism for synthesizing a deuterated triazole derivative of phosphitylated thymidine must be found[18].

2 INTRODUCTION & HISTORICAL BACKGROUND

2.1 DNA STRUCTURE AND BACKBONE DYNAMICS

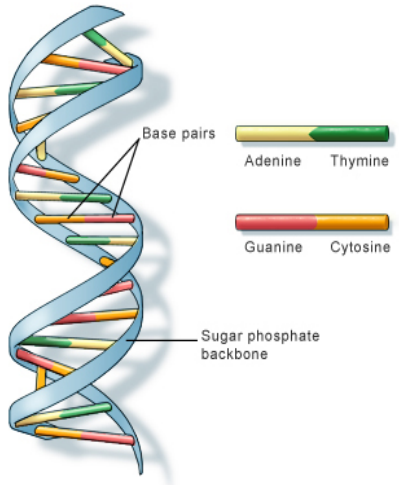

Fig 2.1.1 DNA Double Helix A molecular model of the DNA double helix showing the sugar phosphate backbone as ribbons and the bases as stick models[2]

We are all familiar with Watson and Crick's double helix model, a simple presentation of the links between the paired DNA nucleotides adenosine, guanine, cytosine, and thymine and the sugars and phosphate groups that stitch them together into one polynucleotide chain (see fig 2.1.1)[19]. Human DNA in B form and D-conformation is a repeating nucleoside chain, made up of deoxyribose molecules with heterocyclic bases substituted at their C1' positions- thymine, adenine, guanine, or cytosine. Chains are vertically linked by phosphodiester bonds to form strands, which in turn are bound in double strands by hydrogen bonding between bases [4].

Although the simple model of DNA projects a set of molecules held in stiff bonds and hydrogen bonds, the backbone dynamics of DNA pertain to its broad protein-binding abilities and epigenetic modifications. Enzymes, activators, and repressors must bind DNA for essential functions like DNA replication and transcription (for protein production) to be carried out (see figure 2.1.2). Many models of internal dynamics have been presented, which over the course of time have increasingly embraced two-site jumps, twisting (changes in the azimuthal angle between nuclei), wobbling, and, most importantly, torsion [4, 20-23].

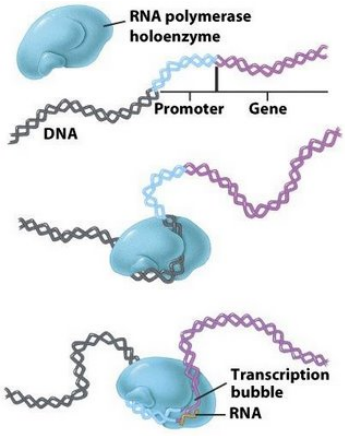

Fig 2.1.2. RNA Polymerase binds to a welcoming DNA strand and begins transcription [3].

Epigenetic modifications are those modifications to the genome that affect gene expression but are not strictly the DNA code. They include acetylation of both histones and DNA, as well as DNA methylation [24].

2.2 DNA METHYLATION

In epigenetic research, DNA methylation is one of several events, also including histone methylation and phosphorylation, that effect genetic modifications to yield imprinting and dictate chromatin stability[25-27]. In short, DNA methylation helps the cell control the expression and function of genes, and, therefore, specific site identification *and* genome-wide methylation levels offer insight into problems stemming from gene regulation (cancer, for instance). Accordingly, a wave of research focused upon its completion, detection, and involvement in disease diagnostic and epigenetics. DNA methylation is the addition of a methyl group (-CH_3) onto a nucleotide; the exact mechanism differs depending on the nucleotide (see Fig 2.2.1).

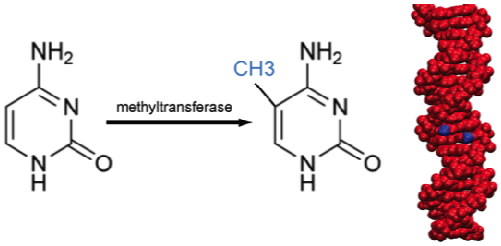

Fig 2.2.1 Unmethylated and methylated forms of single nucleotide cytosine[1]. Methyltransferases catalyze this shift in vivo.

Methylation of cytidine replaces an individual proton with a larger methyl group. As such, it posits a proton near a backbone oxygen, facilitating the formation of the hydrogen bond between the backbone oxygen and a methyl proton [18]. Previous studies have shown that C9 methylation quenches the dynamics of the otherwise highly mobile backbone and sugar moieties at C9 [18]. Although this is an emerging area of study, the existence of a C-H...O bond (much weaker than traditionally defined hydrogen bonds) is supported by the crystallographic studies of Timsit and co-workers, who analyzed the hydration patterns of nucleic acids to conclude that intranucleotide hydrogen bonds are conserved in aqueous environments after methylation [28]. These bonds may restrict motion and thus the ability of certain proteins to bind to the DNA (proteins which depend on the give present in un-methylated DNA in order to bind).

Although much of the research thus far in this field has been comprised mostly of solution NMR, liquid environments offer only peaks which are averages of a series of motions. Solid-state H2-NMR

will reveal the dynamics of the C9 methyl rotation by probing the methyl group directly, yielding a more accurate picture of what is happening at the methylation site molecule. This analysis will clarify the relationship between DNA methylation function and structure by determining whether or not this specific CH---O hydrogen bond , between C9 and G4, quenches dynamics and how that affects the overall structure of the molecule.

2.3 THEORY - SOLID-STATE NMR

All types of spectroscopy have a few common characteristics. They require a source of electromagnetic radiation (EMR). This radiation may be quantized by considering the wave-particle duality of any energetic release/absorption. Well-defined nuclear states (or stationary states) exist and can be quantized only when there are no time-dependent perturbations to the system (no environmental changes). These stationary states have quantized energies and thus so do the transitions between them. Any source of EMR can also be considered as a wave with calculable velocity, wavelength, and frequency. Wave-particle duality in quantum mechanical terms means that each atom in a molecule is treated as a quantum oscillator [29]. When multiple quantum oscillators are treated with the same EMR, their energy will decay by different degrees over time. Their wave functions are of the form $A=A_o[\cos(\omega t+\Phi)]e^{-kt}$ but each particle affected will have its own wave function with its own decay constant, k. The inverse of this constant is the relaxation time of the decay process for the change in A from A_o to A_o/e. This is an example of damped harmonic oscillation, whose decay depends on the being described by multiple frequencies [29]. Mathematically, this represents a small jump from the treatment of harmonic oscillators. Finally, any spectrometer will have a resolution limit, which is expressed in frequency for nuclear magnetic resonance (NMR) [30]. Any two transitions separated by less than the resolution limit will be indistinguishable [30]. Perfection of spectroscopic technique in different frequency ranges has bred the many forms of spectroscopic analysis available to modern scientists. Although there is reasonably large range of frequencies detectable by NMR, it depends primarily on lower frequencies (radio waves on the order of 30 kHz to 300 GHz) in order to capture electronic transitions/nuclear spin interactions (discussions on these to come).

Nuclear magnetic resonance is a simple concept with complicated execution, especially in the solid state. At its core, the technique combines an appropriate source of radiofrequency EMR and a

powerful magnet capable of inducing a strong and uniform magnetic field [31]. As mentioned, each atom in a molecule is treated as an atomic oscillator. NMR uses a sample's response to a magnetic field, B_{app}, to analyze it. Precession in the magnetic field is caused by spin properties of the electrons attached to each atomic oscillator. The energy of the magnetic moment μ, of an electron in an applied magnetic field, B_{app}, can be quantified by the Hamiltonian:

$$\hat{H}=-\mu B_{app}=-\gamma_e B\hat{l} \qquad \text{Eq. 1}$$

where l is the orbital angular momentum operator and

$$\gamma_e=\frac{-e}{2m_e} \qquad \text{Eq. 2}$$

is the magnetogyric ratio of the electron [29]. The negative sign in these equations reflects that the electron spin is antiparallel to it orbital angular momentum. The dependence of a nucleus' resonance frequency on its local electronic environment causes chemical shift. The induced local field around a proton, B_{loc}, interacts with the applied field, B_{app}, to create a unique nuclear field. If they are in the same direction, then the B_{eff} felt by the nucleus will be greater than the applied field itself and the nucleus is "deshielded" and their resonances are "downfield." If they are in opposite directions, then the reverse is true and the nucleus is "shielded" and "upfield" [29] (see Figure 2.3.1). This concept can be mathematically described, such that B_{loc} is related to B_{app}:

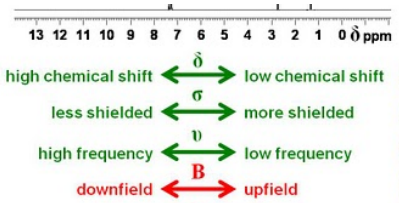

Figure 2.3.1: The NMR scale

$$B_{loc}=B_{app}+\delta B_{app}\ [T] \qquad \text{Eq. 3}$$

where δB_{app} represents the additional magnetic field affecting the nuclei due to the induced orbital

angular momentum of the local field:

$$\delta B_{app}=-\sigma B_{app}\ [T] \qquad \text{Eq. 4}$$

where σ is the shielding constant [29]. A given shielding constant is specific to the atom it represents and the functional group it is in. Due to these multiple dependencies, shielding constants tend to be difficult to determine. Equations 4 and 5 make it clear that the orientation of a molecule relative to B_{app} is important. Logically, this can be defined by the idea that the precession of electrons normal to the applied field are limited to the shapes of their orbitals. A π orbital greatly affects chemical shifts of nearby nuclei when perpendicular to the applied field. A sigma bond (the precession of a carbon-carbon bond) affects the molecule most when it is parallel to the applied field [29]. Chemical shift anistropy can be defined as the difference between the chemical shift of an atom in an isotropic state and in an anisotropic state-that is to say, **n**uclei which are part of a molecule or are in a particular functional group will resonate at different frequencies depending on shielding by the local electronic environment due to orientation in the molecule [32]. Chemical shift anisotropy is especially important in solid-state NMR. The relationship between the observed resonance frequency of nucleus, i, and an applied field can be quantified by:

$$\nu_i=\gamma B_o(1-\bar{\sigma}_i)\ \ [Hz] \qquad \text{Eq. 6}$$

where $\bar{\sigma}_i$ is known as the "shielding tensor." Because of its dependence on the shielding tensor, chemical shielding is thus known as a second -rank tensor. Chemical shift can thus be defined by:

$$\delta=\frac{\nu_i-\nu_o}{\nu^o}(10^6)\ \ [Hz] \qquad \text{Eq. 7}$$

where ν^o is the resonant frequency of a given reference compound. Note that this definition is independent of the applied field since both the numerator and denominator depend upon it equally.

The same concept can be equally represented by the Hamiltonian:

$$E_{CS}=-\hbar\gamma I\cdot B_{ind},\quad B_{ind}=\bar{\sigma}\cdot B_{app} \qquad \text{Eq. 8}$$

The effects of the field on the nuclei being studied is measured by the application of pulses to the sample [31]. An applied pulse will induce a shift in each nuclei, which then relaxes back to its equilibrium position. This time is its relaxation time. Several different forms of the relaxation time may be quantified, generally by fitting collected data to a known equation that includes the relaxation time in an exponent and solving [31].

The last important point of NMR theory to discuss is coupling. The fundamental cause of coupling is the interdependence of multiple quantum oscillators in the same molecule for their expressed frequencies [29]. The splitting of resonances into individual lines- known as the fine structure of the spectrum-happens as each magnetic nucleus affects the local field of its neighbors and thus slightly modifies their expressed frequencies. J-coupling, or dipolar coupling, is propagated by interactions of nuclear spin with the spins of bonding electrons (think of the sigma bonds discussed above). Solid-state techniques tend to minimize or eliminate the significance of coupling. The dipolar coupling between two nuclei is inversely proportional to the cube of their distance. This has the effect that the polarization transfer mediated by the dipolar interaction is cut off in the presence of a third nucleus (all of the same kind, e.g. ^{13}C) close to one of these nuclei. This effect is commonly referred to as dipolar truncation. It has been a major obstacle in determination of internuclear distances in solution NMR and recoupled SSNMR [5]. By means of labeling schemes or pulse sequences, however, it has become possible to circumvent this problem in a number of ways [33, 34]. In the case of this thesis, coupling is rendered insignificant by the use of deuterium.

Any nucleus of spin quantum number I=1/2 (as in ^{1}H, ^{13}C, ^{15}N, and ^{31}P) has spherical charge distribution [5]. Nuclei with spin quantum numbers greater than this (as in ^{2}H, ^{17}O) have an asymmetric distribution - this is described as a nuclear electric quadrupolar moment (eQ). In other words, eQ represents the departure of the nuclear charge distribution from spherical symmetry. Quadupolar nuclei interact with their electronic surroundings to result in larger splitting of peaks.

The line width of a spectrum is determined by both direct magnetic dipolar interaction between nuclear spins and the chemical shifts of the molecules in the solid state (do not average out to zero except when placed at the magic angle).

2.4 THEORY - DEUTERIUM IN NMR

Deuterium is heavy hydrogen, that is, it contains one extra neutron compared to hydrogen; its nucleus is called a deuteron. Deuterium does indeed have a quantum number greater than 1/2. The Hamiltonian for the deuteron can be written:

$$\hat{H}=-\frac{\hbar^2}{2\mu}\nabla^2 + V \qquad \text{Eq. 8}$$

where the entire first term is kinetic energy of the molecule's center of mass and V is the potential energy due to the interaction of the molecule's nuclei[35].

Its quadrupole moment is $eQ=0.286 \times 10^{-26}$ cm^2, and its Pake doublet can be evaluated using:

$$v_{ZZ} = \tfrac{1}{2}\delta(3\cos^2\theta-1) \qquad \text{Eq. 10}$$

$$v_{zz} = -\tfrac{1}{2}\delta(3\cos^2\theta-1) \qquad \text{Eq. 11}$$

where $$\delta = (\tfrac{3}{4})\left(\frac{e^2qQ}{h}\right) = \Delta v_{doublet} \qquad \text{Eq. 12}$$

which gives the QCC= e^2qQ/h for a C-^{2}H bond, generally ranging from 160-210 kHz [5]. The Pake doublet is a mirror image, one from the -1◄►0 transition (Eq. 10) and from the 0◄►1 transition (Eq. 11) (see fig. 2.4.1, from Alam and Drobny's seminal work on the topic of solid-state NMR studies of DNA) [4]. In the course of this experiment, we replaced the three hydrogen atoms in one methyl group with deuterium, so that we could track the dynamics of that methyl side group.

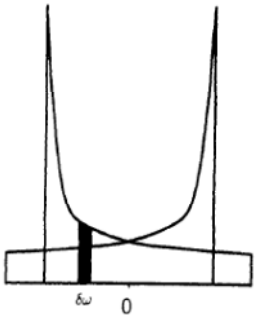

Fig 2.4.1 Deuterium NMR solid sample Pake doublet [4]

3 EXPERIMENTAL METHODS

3.1 SYNTHESIS OF DEUTERATED TRIAZOLE DERIVATIVE OF PHOSPHITYLATED THYMIDINE

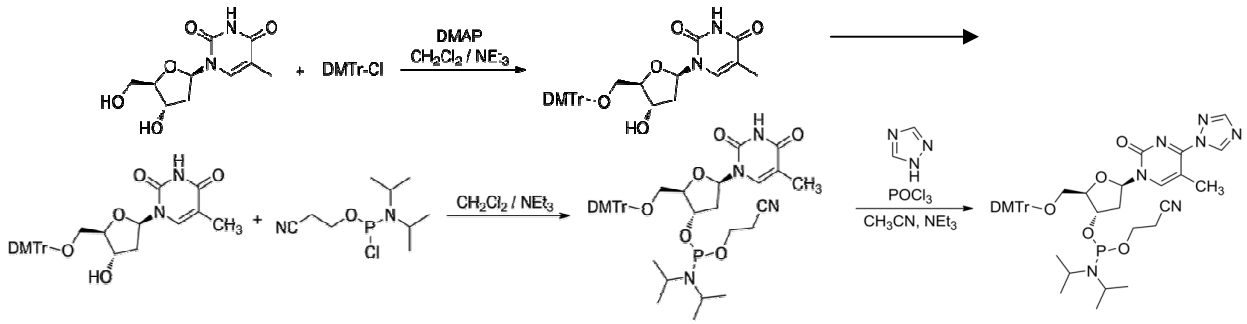

Fig 3.1.1. Reaction Mechanism for Synthesis of Triazole Derivative of Phosphitylated Thymidine.

All initial thymidine and reactants were Sigma Aldrich. First, thymidine was deuterated and purified by column. It was verified by ^{1}H NMR. This first-stage product was then tritylated to protect its 5'-hydroxyl (its primary alcohol) group during the phosphitylation step. This step was catalyzed by dimethylaminopyridine, a useful base and nucleophile due to the electron donation from its tertiary ring; the reaction may proceed via the formation of an ion complex involving a positively charged nitrogen and chloride ion. This intermediate was verified by solution-state ^{1}H NMR.

This alcohol-protected product was then phosphitylated using the N,N-diisopropylethylamine, a chlorophosphite which is highly reactive toward alcohols. Reaction product was detected by TLC, and confirmed by NMR: it was this step that makes the product very sensitive, in several ways. Firstly, the phosphoramidite product is highly sensitive to water and oxygen, which necessitated the maintenance of argon over the product. This was very difficult to maintain without a glove box, especially given the number of transfers necessary after the phosphitylation. Due to this sensitivity, the product broke down fairly quickly after this step, even though another reaction step and purification was needed before the final product could be shipped off for incorporation into DNA. Secondly, the product was heat-sensitive, which prevented application of strong heat to pull off solvents/byproducts.

The first half of the phosphoramidite was purified via column chromatography. A 100-200 mesh silica slurry was used to about 11 cm in a large column. The eluents used were a 45:45:10 EtOAc:CH_2Cl_2:TEA with an ascending methanol content up to but not exceeding 2%. Collected fractions were checked by TLC, then collected into a large round-bottom and rotovapped down. The sample was put under high vacuum overnight, but was taken down in dichloromethane and once again rotovapped and put under high vacuum. Ultimately, this column purification was decided to be too harsh upon the sensitive product, and eliminated from the synthesis.

The un-columned sample was taken through the next reaction step-the synthesis of a 1,2,4-triazole derivative. The phosphoramidite was first dissolved in acetonitrile. Then, NEt_3 and $POCl_3$ were added. 1,2,4-triazole was added last (reaction 'clock' was started at the addition of the triazole). Product was verified by TLC. Sample was allowed to react at room temperature for approximately 19 hours. It was rotovapped down and massed. It was concluded from the NMR taken this phosphoramidite that there was both product and byproduct(s) present in the mixture.

The TLC of the columned phosphoramidite looked very pure (not shown). The NMR of the purified triazole product made from unpurified phosphoramidite showed little or no product. It was concluded that the byproducts and side reactions present in the round bottom either overshadowed the product in the spectra or actually destroyed it. More importantly, this meant that a taking the raw phosphoramidite through the triazole derivative synthesis uncleaned is not a viable way to avoid product loss due to column chromatography. It was decided that the same extraction used to clean the triazole (5:1 ethyl acetate:TEA followed by 5% Na_2CO_3, drying over Na_2SO_4, and co-evaporation with toluene) would be sufficient.

The NMR of the purified compound showed product and looked very clean aside from the continued presence of TEA in the sample. It is therefore concluded that another base should be tested as a possible substitute, since even high-powered vacuum and co-evaporation with toluene

have failed to fully pull off this base to yield a truly pure product. Hünig's base (N,N-diisopropylethylamine) was tested as a possible substitute for TEA in the phosphitylation step (the reaction of 5'-O-DMT-thymidine to its phosphoramidite) and performed fairly well, so it was tested and chosen as a substitute here as well.

Given the decision to eliminate the column purification and the presence of TEA in the sample, small-scale side-by-side runs of the phosphitylation step were run using acetonitrile and dichloromethane. The raw product from the reaction run in DCM was whitish-clear, while the one in acetonitrile was yellow, thick and obviously much less clean. Although the stated goal of this experiment was to identify the better yield, it was also very important to choose the solvent that lends itself to yielding a final product that is completely cleaned of other chemicals. The largest problem with phosphitylation in previous weeks has been the ability to pull off the base that is used to protect the developing product from the hydrochloric acid evolved in these reaction steps. A switch from triethylamine to anhydrous N,N-diisopropylethylamine much improved the situation, but the level of base or other byproduct in the acetonitrile run was prohibitively high. An equal amount of raw product was used to make each NMR solution and both were run. The size of the product peaks relative to the solvent peak was greater in the DCM run, indicating how much cleaner its phosphoramidite was (a higher portion of the raw product was pure). It was concluded that the risk of not being able to pull off the base in the acetonitrile reaction mixture outweighed the potential for its higher yield. The final yield is only important in that at least 100 mg of final, pure product must be collected. The product absolutely must come out clean. The final deuterated run phosphitylation was run in DCM.

The final run of this synthesis was run in summer 2012 in coordination with Dr. Len Mueller's lab at the University of California, Riverside, in particular by Ryan Kudla.

3.2 SOLID-STATE NMR ANALYSIS

Once the deuterated, methylated nucleotide was successfully synthesized at the UCR lab, it was coupled into the Dickerson sequence by Alpha DNA (Montreal, Quebec, Canada). The result was a 52 milligram sample of $d(CGCGAATTCGCG)_2$, a stable C9-methylated (the methyl group being CD_3) DNA dodecamer which was safe at room temperature. The Na-DNA solid sample was salted to 5% mass content using anhydrous sodium chloride, then washed three times in deuterium-depleted water, frozen and lyophilized. The dry sample was packed into a sample container for the solid-state probe - a plastic tube 1.5 inches in length with removable plugs in each end.

WM Keck Science Department's 500 MHz NMR with a solid-state probe was used to obtain a scan of the dehydrated sample. The resultant spectra represents an overlay of 248,515 scans beginning September 21, 2012 with delay time of 10 μs. Signal was detected and acquisition settings established using a purchased, deuterated polyacrylamide.

After a dehydrated spectrum was obtained, the sample was hydrated to 75% humidity using a sodium chloride chamber with deuterium-depleted water, such that W=10.6 water molecules per molecule of DNA. A new scan was begun October 27, 2012, with a delay time=30 μs, representing an overlay of 164,837 scans. A 93% chamber with potassium nitrate and deuterium-depleted water was prepared but is not in use. The sample is currently in the 75% chamber though its continued use is not anticipated, as will be discussed.

4 RESULTS

4.1 SOLUTION STATE NMR AND TLC VERIFICATION OF SYNTHESIS STEPS

The alcohol protection step and its product's successful conversion into a phosphoramidite were verified by TLC and solution-state NMR. Samples were run at room temperature and under argon.

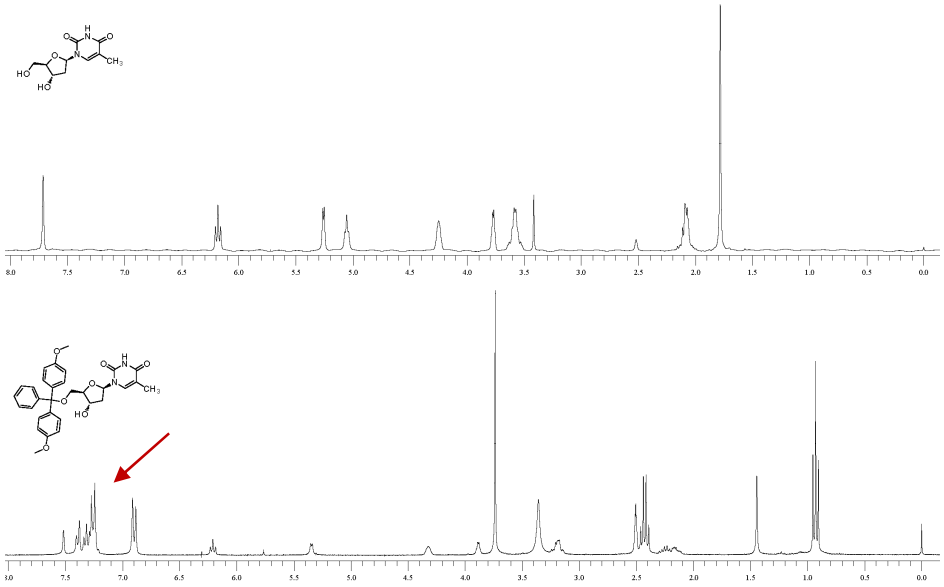

Fig 4.1.1 Solution State 1H NMR stacked scans confirmed the success of the DMTr alcohol protection step. The appearance of the downfield overlapping peaks (red arrow) indicates presence of aromatic rings interacting with one another.

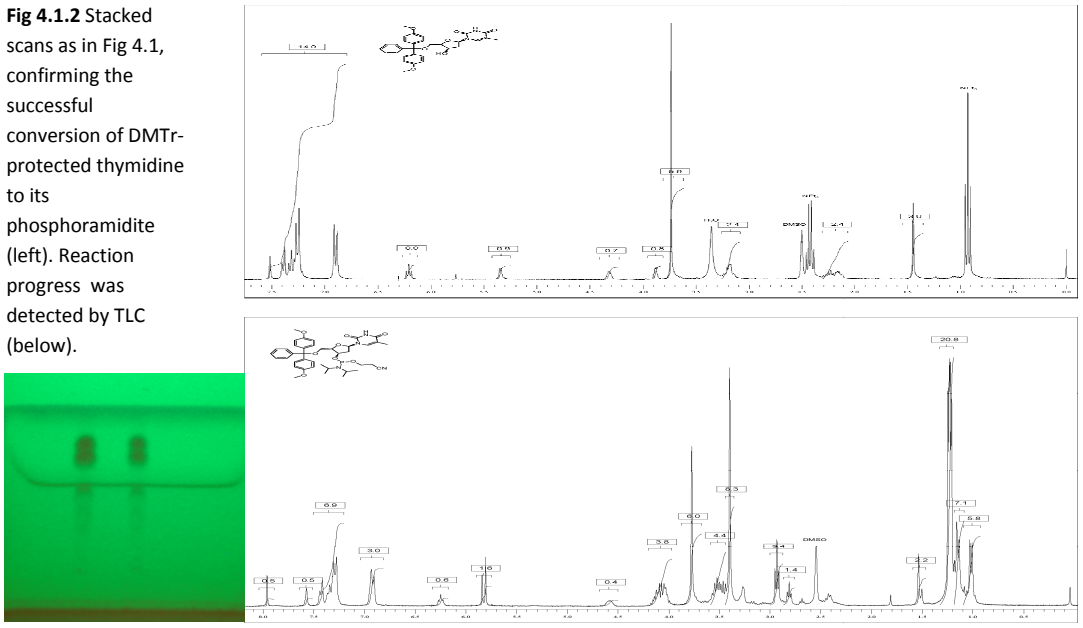

Fig 4.1.2 Stacked scans as in Fig 4.1, confirming the successful conversion of DMTr-protected thymidine to its phosphoramidite (left). Reaction progress was detected by TLC (below).

The NEt_3 and $POCl_3$ were added, followed by 1,2,4-triazole. The reaction was allowed 19 hours at room temperature under argon.

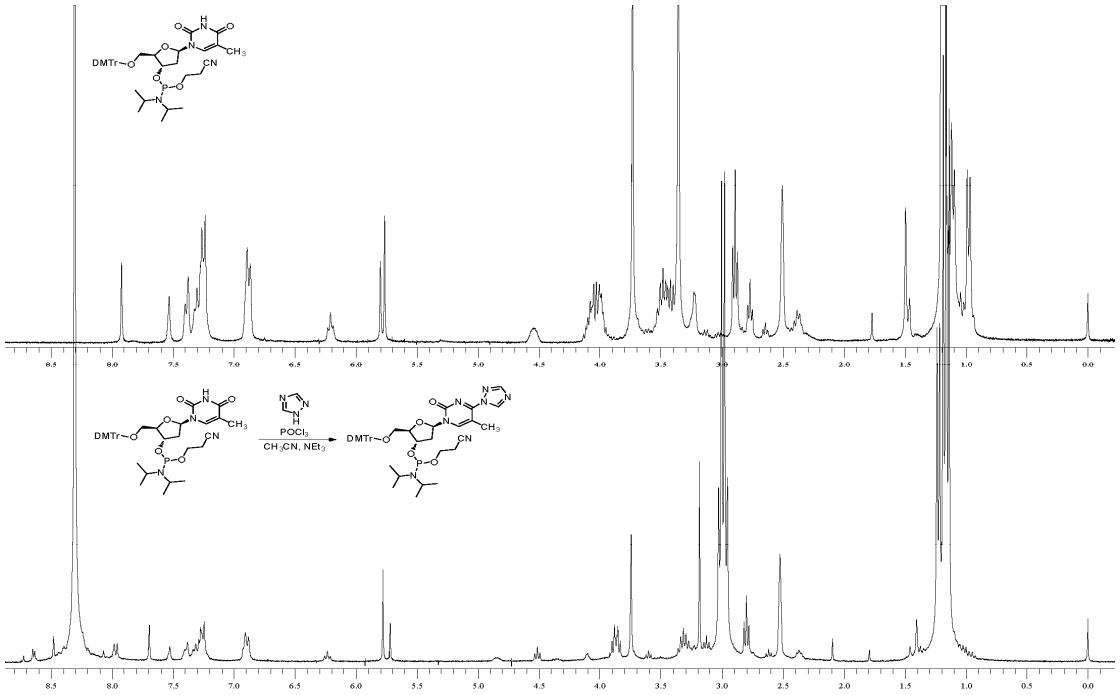

Fig 4.1.3 Stacked scans as in Fig 1 and Fig 2, confirming that the triazole derivative of the thymidine phosphoramidite was synthesized.

4.2 DNA TREATMENT

Immediately following completion of the synthesis, the sample was iced and mailed off to Alpha DNA. The coupled DNA sample that resulted was the Dickerson sequence with its C9 position substituted with our modified nucleotide, with characteristics as shown in Table 1 below.

Table 1: Synthesized C9 Methylated DNA sample

OD-260	1581.1
Micrograms	52082
Picomoles	14282972
Nucleotides	
A	16.67%
C	25%
G	33.33%
T	16.67%
Modified	8.33%
A+T	33.33%
G+C	58.33%
Tm (using %GC)	52.58^{o}C

4.3 ANALYSIS OF METHYLATED DICKERSON DODECAMER

The sample was shipped to KSD with some salt and counter ions present, but was further salted to reach 5% mass content. The salted sample was taken down in deuterium-depleted water repeatedly, and the spectra resulting from the scan is in the following figure:

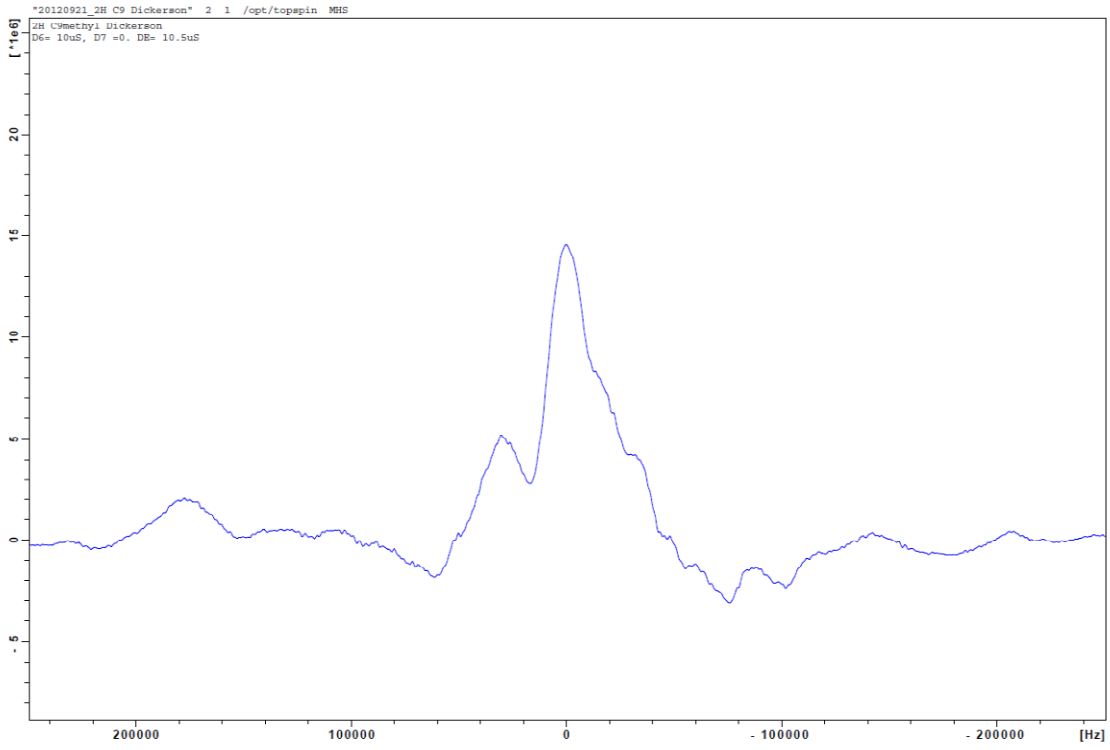

Fig 4.3.1 Dehydrated Methylated Dickerson Dodecamer. 200,000 scans, delay time=

Hydration of the sample in the chamber gave the following results. The theoretical and experimental water contents were calculated.

Table 2 : Hydration of Methylated DNA Sample

% Hydration	Theoretical W (mol H_2O/mol DNA)	Experimental W (mol H_2O/mol DNA)
0	1.4*	Unknown
75	9.8-10.0*	10.6
93	22.6*	--

*Theoretical values from Alam and Drobny, 1991, who reprinted with ACS permission

Hydrated sample was scanned 164,837 times with delay time=30 µs. The following spectra resulted.

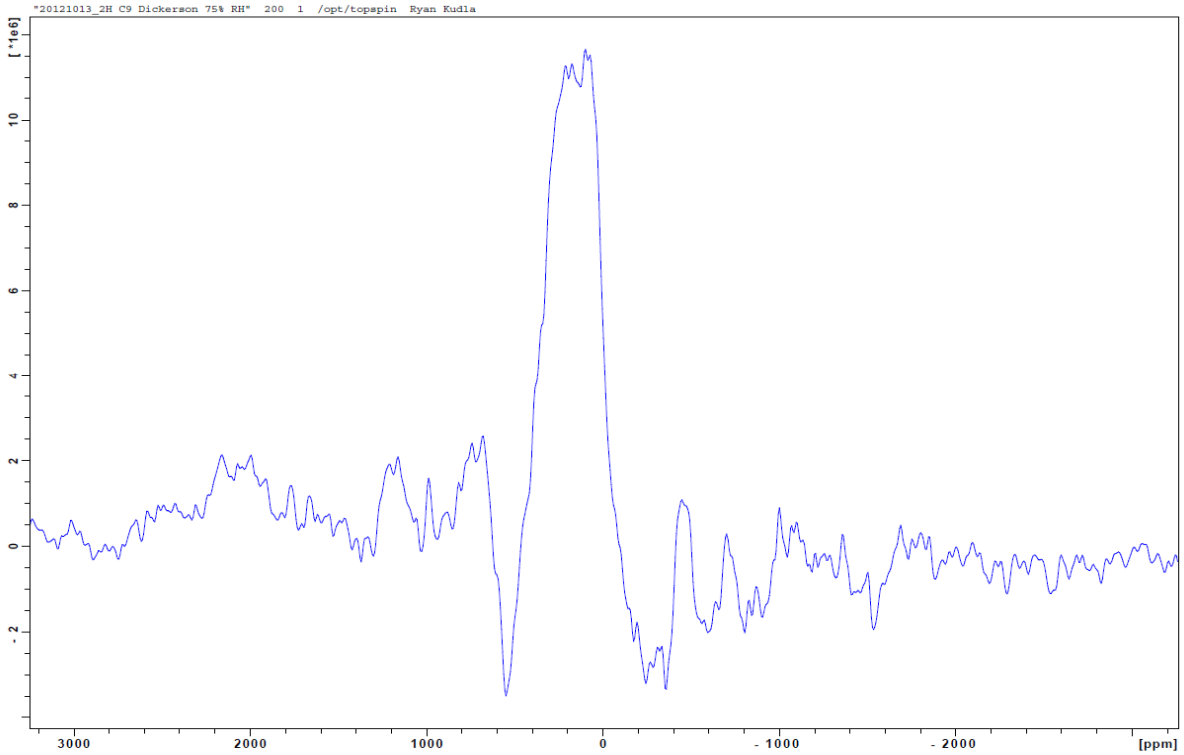

Fig 4.3.2 RH=75% Spectra of Methylated Dickerson Dodecamer, delay time=30 µs.

5 DISCUSSION

5.1 DISCUSSION OF RESULTS

Synthesis of the deuterated, methylated phosphoramidite derivative of thymidine was clearly successful. Although optimization of undeuterated runs was progressive, the synthesis leading to these two scans provided only 52 mg coupled DNA. It was deemed likely before synthesis that at least 100 mg would be needed for a strong solid-state NMR signal. This seems to be the case, since the dehydrated signal was low and the 75% hydrated scan signal even lower. Several factors other than sample size may have contributed to this issue.

Firstly, incomplete deuteration of the thymidine (pre-synthesis step) would have reduced the signal to sample mass ratio regardless of sample size, although this problem might be rendered unnoticeable with a sufficiently large sample. Second, the sample container's seal is insufficient: the plastic tube is built with removable plugs which must be screwed in and tightened but which did not prevent water loss. The 75% hydrated scan produced a spectra with what appeared to be two sets of doublet horns; however, it was actually one low-signal doublet which had shifted out of phase with itself over the course of scanning, presumably due to significant water loss. Massing the sample confirmed this loss. Third, the delay times set on both the dehydrated and hydrated samples were not long enough to gather a good signal. Drobny reported approximately 50 μs delay times, and these scans had 10 μs and 30 μs delays, respectively[4].

Effects on rate motion in the solid state due to hydration levels are clearly evident-the scans presented different shapes. However, given the changing hydration levels, issue with insufficient delay time (which in addition to not being sufficient for either scan, also varied between the two scans), and the sample size, it is not possible to conclude that the difference in these two spectra is experimentally significant. Therefore, it is not possible to comment on evidence for the existence of a CH---O bond based on the data collected here.

5.2 SIMULATED RESULTS & FUTURE WORK

Although the collected data was insufficient to yield relevant comment, simulations run by the Hatcher-Skeers research group have shown promising results worthy of continued investigation of a possible CH---O, which may quench methyl rotation in a solid sample. The group has used three-site jump models using MXET and MXET1 programs, as in Alam and Drobny's analysis and using the interface program the Drobny group developed, Gullringen[36]. At left are two line shape simulations of methyl rotation in DNA. The angle of the deuterated C-D bond is 70^{o} from the helical axis, as established previously[4].

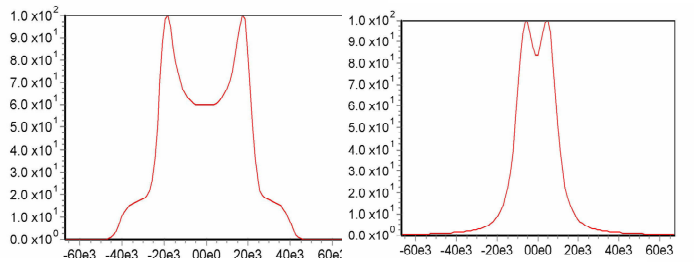

Fig 5.2.1 Simulated methyl rotation using three-site jump model; two axis motion with helix rotation and methyl rotation. On the left, methyl rotation rate = 10^3 Hz (slow), on the right rate = 10^7 Hz (fast); C-D bond at 70^{o} angle to DNA helix axis.

The simulations use two axes of motion to account for the overall motion of the molecule in the magnetic field upon hydration. The Pake doublet width (slow) in this simulation is 55 kHz. From these simulations, it can be concluded that ^{2}H solid-state NMR can differentiate between differing dynamic rotational states (fast versus intermediate/fast rate motion, as shown in the figure). Therefore, continued studies in solid-state NMR are likely to offer insight into the existence of a CH---O bond in DNA helices, since its existence would yield a reduced quadrupolar coupling constant as observed.

.

References:

1. Zou, X.Q., et al., *Recognition of methylated DNA through methyl-CpG binding domain proteins.* Nucleic Acids Research, 2012. **40**(6): p. 2747-2758.
2. Medicine, U.S.N.L.o., *DNA*. 2012, National Institute of Health: Web.
3. Singer, P.W., C.W., *Promoter search by Escherichia coli RNA polymerase on a circular DNA template.* Journal of Biological Chemistry, 1987. **262**: p. 14178-14189.
4. Alam, T.M. and G.P. Drobny, *SOLID-STATE NMR-STUDIES OF DNA-STRUCTURE AND DYNAMICS.* Chemical Reviews, 1991. **91**(7): p. 1545-1590.
5. Saito, H., I. Ando, and A. Naito, *Solid-State NMR for Biopolymers: Principles and Applications*. 2006, Springer-Verlag: Dordrecht, The Netherlands.
6. Wuthrich, K., *NMR of Proteins and Nucleic Acids.* 1986, New York: Wiley-Interscience. 292.
7. Hart, K., et al., *Optimization of the CHARMM Additive Force Field for DNA: Improved Treatment of the BI/BII Conformational Equilibrium.* Journal of Chemical Theory and Computation, 2012. **8**(1): p. 348-362.
8. Hatcher, M.E., et al., *A solid-state deuterium NMR study of the localized dynamics at the C9pG10 step in the DNA dodecamer d(CGCCAATTCGCG) (2).* Journal of the American Chemical Society, 1998. **120**(38): p. 9850-9862.
9. Wu, J.-H., et al., *Identification of DNA methylation of SOX9 in cervical cancer using methylated-CpG island recovery assay.* Oncology reports, 2013. **29**(1).
10. Poeta, M.L., et al., *Aberrant promoter methylation of beta-1,4 galactosyltransferase 1 as potential cancer-specific biomarker of colorectal tumors.* Genes Chromosomes & Cancer, 2012. **51**(12): p. 1133-1143.
11. Dickerson, R.E. and H.R. Drew, *STRUCTURE OF A B-DNA DODECAMER .2. INFLUENCE OF BASE SEQUENCE ON HELIX STRUCTURE.* Journal of Molecular Biology, 1981. **149**(4): p. 761-786.
12. Huang, W.C., et al., *A SOLID-STATE DEUTERIUM NMR-STUDY OF FURANOSE RING DYNAMICS IN D(CGCGAATTCGCG) 2.* Journal of the American Chemical Society, 1990. **112**(25): p. 9059-9068.
13. Kintanar, A., et al., *DYNAMICS OF BASES IN HYDRATED D(CGCGAATTCGCG) 2.* Biochemistry, 1989. **28**(1): p. 282-293.
14. Bax, A. and L. Lerner, *MEASUREMENT OF H-1-H-1 COUPLING-CONSTANTS IN DNA FRAGMENTS BY 2D NMR.* Journal of Magnetic Resonance, 1988. **79**(3): p. 429-438.
15. Zhu, L., *Dissertation*, in *Chemistry*. 1994, University of Washington.
16. Holbrook, S.R., et al., *LOCAL MOBILITY OF NUCLEIC-ACIDS AS DETERMINED FROM CRYSTALLOGRAPHIC DATA .2. Z-FORM DNA.* Journal of Molecular Biology, 1986. **187**(3): p. 429-440.
17. Withka, J.M., et al., *TOWARD A DYNAMIC STRUCTURE OF DNA - COMPARISON OF THEORETICAL AND EXPERIMENTAL NOE INTENSITIES.* Science, 1992. **255**(5044): p. 597-599.
18. Lin, V., *Synthesis of deuterated 5-methylcytodine for incorporation into DNA oligomers*, in *Chemistry*. 2010, Scripps College: Claremont, CA.
19. Watson, J.D. and F.H.C. Crick, *Molecular structure of nucleic acids - A structure for deoxyribose nucleic acid (Reprinted from Nature vol 171, pg 737, 1953).* Clinical Orthopaedics and Related Research, 2007(462): p. 3-5.
20. Allison, S.A., E.L. Chang, and J.M. Schurr, *EFFECTS OF DIRECT AND HYDRODYNAMIC-FORCES ON MACROMOLECULAR DIFFUSION.* Chemical Physics, 1979. **38**(1): p. 29-41.
21. Allison, S.A. and J.M. Schurr, *TORSION DYNAMICS AND DEPOLARIZATION OF FLUORESCENCE OF LINEAR MACROMOLECULES .1. THEORY AND APPLICATION TO DNA.* Chemical Physics, 1979. **41**(1-2): p. 35-59.

22. Bolton, P.H. and T.L. James, *MOLECULAR MOTIONS IN RNA AND DNA INVESTIGATED BY P-31 AND C-13 NMR RELAXATION.* Journal of Physical Chemistry, 1979. **83**(26): p. 3359-3366.
23. Hogan, M.E. and O. Jardetzky, *EFFECT OF ETHIDIUM-BROMIDE ON DEOXYRIBONUCLEIC-ACID INTERNAL MOTIONS.* Biochemistry, 1980. **19**(10): p. 2079-2085.
24. Weaver, R., *Molecular Biology*. 5 ed. 2011, New York: McGraw-Hill.
25. Heyn, H. and M. Esteller, *DNA methylation profiling in the clinic: applications and challenges.* Nature Reviews Genetics, 2012. **13**(10): p. 679-692.
26. Garcia-Gimenez, J.L., et al., *Epigenetic biomarkers: A new perspective in laboratory diagnostics.* Clinica Chimica Acta, 2012. **413**(19-20): p. 1576-1582.
27. Heichman, K.A. and J.D. Warren, *DNA methylation biomarkers and their utility for solid cancer diagnostics.* Clinical Chemistry and Laboratory Medicine, 2012. **50**(10): p. 1707-1721.
28. Mayer-Jung, C., D. Moras, and Y. Timsit, *Hydration and recognition of methylated CpG steps in DNA.* Embo Journal, 1998. **17**(9): p. 2709-2718.
29. Pochapsky, T.C. and S.S. Pochapsky, *NMR for Physical and Biological Scientists*. 2007, New York: Taylor and Francis.
30. Laws, D.D., H.M.L. Bitter, and A. Jerschow, *Solid-state NMR spectroscopic methods in chemistry.* Angewandte Chemie-International Edition, 2002. **41**(17): p. 3096-3129.
31. Atkins, P., J.d. Paula, and R. Friedman, *Quanta, Matter, and Change: A Molecular Approach to Physical Chemistry*. 2009, New York: W.H. Freeman and Co.
32. Schaefer, J., *CHARACTERIZATION OF IMPACT STRENGTH OF GLASSY POLYMERS BY MAGIC-ANGLE C-13 NMR.* Bulletin of the American Physical Society, 1976. **21**(3): p. 443-443.
33. Duer, M.J., *Introduction to Solid-State NMR Spectroscopy*. 2004, Blackwell: Oxford.
34. Shewmaker, F., et al., *The Functional Curli Amyloid Is Not Based on In-register Parallel beta-Sheet Structure.* Journal of Biological Chemistry, 2009. **284**(37): p. 25065-25076.
35. Wong, S.S.M., *Introductory Nuclear Physics*. 2008, New York: Wiley. 472.
36. Meints, G.A., T. Karlsson, and G.P. Drobny, *Modeling furanose ring dynamics in DNA.* Journal of the American Chemical Society, 2001. **123**(41): p. 10030-10038.